

# The homogeneous $B_1$ model as polynomial eigenvalue problem

Daniele Tomatis<sup>a,\*</sup>, Johan Cufé<sup>b</sup>

<sup>a</sup>*DES, Service d'études des réacteurs et de mathématiques appliquées (SERMA),  
CEA, Université Paris-Saclay, F-91191 Gif-sur-Yvette, France*

<sup>b</sup>*Dipartimento di Ingegneria Astronautica, Elettrica ed Energetica  
Università La Sapienza, 00186 Roma, Italy*

---

## Abstract

The homogeneous version of the  $B_1$  leakage model is a non-linear eigenvalue problem which is generally solved iteratively by a root-finding algorithm, combined to the supplementary eigenvalue problem of the multiplication factor. This problem is widely used for ordinary cross section preparation in reactor analysis. Our work approximates this problem with a polynomial eigenvalue problem, which can be easily transformed into an ordinary linear generalized eigenproblem of size equal to the initial one multiplied by the polynomial degree used for the approximation of a transcendental function. This procedure avoids recurring to numerical root-finding methods supported by extra eigenvalue problems. The solution of the fundamental buckling with increasing approximation order is compared to the reference value obtained by inverse iterations.

*Keywords:* Leakage model, neutron transport, homogeneous  $B_1$

---

## Contents

<b>1</b>	<b>Introduction</b>	<b>2</b>
<b>2</b>	<b><math>B_n</math> Theory</b>	<b>3</b>
<b>3</b>	<b>Homogeneous <math>B_n</math></b>	<b>4</b>

---

\*Corresponding author. Tel.: +33 1 69 08 39 79.

Email address: [daniele.tomatis@cea.fr](mailto:daniele.tomatis@cea.fr) (Daniele Tomatis)

<b>4</b>	<b>Homogeneous <math>B_1</math></b>	<b>5</b>
4.1	Multigroup Homogeneous $B_1$ . . . . .	7
4.2	The Polynomial Eigenvalue Problem . . . . .	9
4.3	Non-linear Inverse Iterations . . . . .	10
<b>5</b>	<b>Numerical Results</b>	<b>12</b>
<b>6</b>	<b>Conclusion</b>	<b>17</b>
<b>Appendix A</b>	<b>Solution of the integrals over the unit sphere</b>	<b>17</b>

## 1. Introduction

Critical configurations of lattice transport calculations are usually achieved by means of a leakage model. These calculations prepare homogenized cross sections in a few energy groups for specific types of fuel elements, to be  
5 stored in external data libraries for later use in full-core calculations. The exact physical conditions of the fuel elements are unknown at the time of library generation, except for the fact that the element will operate in a critical neutron-multiplying environment. In absence of further knowledge, each element is also considered as surrounded by other identical elements,  
10 like constituting a periodic regular grid in all directions which extends to infinity. Such condition reproduces reflection at the boundary, with unitary albedo.

The  $B_n$  approximation of neutron transport is the most used to obtain a fundamental mode associated with a given multiplication factor  $k$  (Hébert, 2009). The model is briefly introduced in section 2, as in Hébert's textbook.  
15 In practice, leakage rates per group are varied until matching criticality. Mathematically, it yields a new nonlinear eigenvalue problem whose solution is traditionally sought iteratively in combination with the generalized eigenvalue problem of the multiplication factor. Specifically, a root-finding  
20 algorithm is employed to converge on a given eigenvalue  $B^2$ , representing the curvature (or inflection point) of the flux on a macroscopic scale, while the power method resolves at each iteration a new generalized  $k$ -eigenvalue problem for a fixed value of  $B^2$  until matching the unitary multiplication factor. The solution of several and different  $k$ -eigenvalue problems are then needed  
25 to obtain the fundamental eigenpair. In this work, we propose a different solution method using a single linear eigenvalue problem that can still be

solved efficiently by the power method. This new eigenvalue problem comes from an approximation of the initial problem and it avoids the use of root-finding methods. Finally, nonlinear inverse iterations are introduced to solve the original problem and to verify the numerical solution of the polynomial eigenvalue problem.

## 2. $B_n$ Theory

The time-independent neutron transport equation writes:

$$[\mathbf{\Omega} \cdot \nabla + \Sigma(\mathbf{r}, E)] \phi(\mathbf{r}, E, \mathbf{\Omega}) = \int_0^\infty dE' \left[ \int_{4\pi} d\mathbf{\Omega}' \Sigma_s(\mathbf{r}, E \leftarrow E', \mathbf{\Omega} \leftarrow \mathbf{\Omega}') \phi(\mathbf{r}, E', \mathbf{\Omega}') + \frac{\chi(E)}{4\pi k} \nu \Sigma_f(\mathbf{r}, E') \phi(\mathbf{r}, E') \right], \quad (1)$$

where  $\Sigma$  is the total macroscopic cross section,  $\Sigma_s$  is the differential scattering macroscopic cross section,  $\nu \Sigma_f$  is the fission production macroscopic cross section and  $\chi$  is the neutron emission spectrum. All neutron production is assumed here as prompt. The multiplication factor  $k$  is the eigenvalue of the generalized eigenvalue problem in Eq. 1, corresponding to its companion eigenmode  $\phi$ , which represents the angular flux distribution of neutrons at the position  $\mathbf{r}$  flying along the direction  $\mathbf{\Omega}$  at energy  $E$ . The fission reaction rate uses only the scalar angle-integrated flux because fission is isotropic.

The  $B_n$  theory uses the factorization of the neutron flux  $\phi$  in a component  $\psi$  which is slowly varying in space, that is with respect to the characteristic length of the fuel element, like its pitch, and another one  $\varphi$  which is of faster variation therein:

$$\phi(\mathbf{r}, E, \mathbf{\Omega}) = \psi(\mathbf{r}) \varphi(\mathbf{r}, E, \mathbf{\Omega}). \quad (2)$$

The macroscopic flux  $\psi$  takes only the spatial dependence and satisfies the diffusive homogeneous Helmholtz equation over the scale of the whole reactor:

$$\Delta \psi + B^2 \psi = 0, \quad (3)$$

where  $\Delta = \nabla \cdot \nabla$  is the Laplacian operator and  $B^2$  is the geometrical buckling representing the curvature of the flux. A general solution of Eq. 3 is  $\psi = C \exp(i\mathbf{B} \cdot \mathbf{r})$ , where  $C$  is a constant and the magnitude of the vector  $\mathbf{B}$  is  $|\mathbf{B}| = \sqrt{\mathbf{B} \cdot \mathbf{B}} = B$ .

The microscopic flux  $\varphi$  takes into account the changes of the neutron flux within the fuel element. Although the theory can apply to any kind of fuel element under the aforementioned assumption of periodicity, it is customary to consider a single fuel assembly, especially when preparing homogenized cross sections for reactor calculations by lattice transport computer codes. The core is then supposed as filled by the same unit so that the fuel assembly is calculated by using reflection or periodic boundary conditions. The equation to solve for  $\varphi$  comes from substitution of Eq. 2 in Eq. 1. After assuming that  $\psi > 0$  everywhere and by noticing that  $\nabla\psi = i\mathbf{B}\psi$ , it is:

$$[\mathbf{\Omega} \cdot (\nabla + i\mathbf{B}) + \Sigma] \varphi = q(\varphi), \quad (4)$$

with  $q$  representing all source terms at the right hand side of Eq. 1, but now with the rates as function of  $\varphi$  instead of the angular flux  $\phi$ .

The standard procedure adopted in lattice transport codes is to modify the buckling  $B^2$  until matching a unitary multiplication factor in the source term  $q$ , which means also adjusting the leakage rates in case of insufficient or excessive production of neutrons by fission, i.e. positive or negative  $B^2$ , respectively.

There are two versions of the  $B_n$  model according to the presence of the spatial dependence in the microscopic flux: the homogeneous version and the heterogeneous version.

### 3. Homogeneous $B_n$

The homogeneous model is somewhat simpler to solve, being the preferred option for lattice calculations of LWR fuel assemblies. The microscopic flux is considered as averaged in space, i.e.  $\varphi(E, \mathbf{\Omega})$ , as well as all macroscopic cross sections entering the balance equation. The same cross sections can also be considered as spatially homogenized quantities with reference flux solutions from previous calculations.

After removal of the gradient operator, Eq. 4 provides the starting point. The angular dependence is addressed by expanding the flux on the spherical harmonics functions  $Y$ , which arise in the development of the scattering source in isotropic media on Legendre polynomials of the direction cosine between the incident and exiting directions of collision,  $\mu = \mathbf{\Omega} \cdot \mathbf{\Omega}'$ :

$$\Sigma_s(E \leftarrow E', \mathbf{\Omega} \leftarrow \mathbf{\Omega}') = \frac{1}{2\pi} \Sigma_s(E \leftarrow E', \mu) = \sum_{\ell=0}^L \frac{2\ell+1}{4\pi} \Sigma_{s,\ell}(E \leftarrow E') P_\ell(\mu),$$

with  $L$  as order of scattering anisotropy.  $L$  is given by the available nuclear data library. A complete expansion of the angular flux in spherical harmonics is:

$$\varphi(E, \mathbf{\Omega}) = \sum_{\ell=0}^{\infty} \frac{2\ell+1}{4\pi} \sum_{m=-\ell}^{\ell} \Phi_{\ell}^m(E) Y_{\ell}^m(\mathbf{\Omega}) \quad (5a)$$

with the moments given by

$$\Phi_{\ell}^m = \int_{4\pi} d\mathbf{\Omega} Y_{\ell}^{*,m}(\mathbf{\Omega}) \varphi(E, \mathbf{\Omega}). \quad (5b)$$

The superscript  $*$  denotes complex-conjugation. The source at the right hand side of the neutron balance equation is then rewritten after use of Eqs. 5 and of the addition theorem (Edmonds, 1996):

$$P_{\ell}(\mu) = \sum_{m=-\ell}^{\ell} Y_{\ell}^m(\mathbf{\Omega}) Y_{\ell}^{*,m}(\mathbf{\Omega}'),$$

as,

$$q(E, \mathbf{\Omega}) = \sum_{\ell=0}^{\infty} \frac{2\ell+1}{4\pi} \sum_{m=-\ell}^{\ell} Y_{\ell}^m(\mathbf{\Omega}) \int_0^{\infty} dE' \Sigma_{p,\ell}(E \leftarrow E') \Phi_{\ell}^m(E'), \quad (6)$$

with  $\Sigma_{p,\ell} = \Sigma_{s,\ell}(E \leftarrow E') + \chi(E) \nu \Sigma_f(E') \delta_{\ell 0}$ <sup>1</sup>.

A set of  $(L+1)^2$  equations can be derived by inversion of the streaming plus total collision operator from Eq. 4 on the source from Eq. 6, and weighted integration in angle with the spherical harmonics of order less or equal to  $L$ . The truncation of the spherical harmonics expansion to the order  $n \leq L$  yields finally the  $B_n$  model approximation.

#### 4. Homogeneous $B_1$

The homogeneous  $B_1$  model is very common in lattice calculations for cross section preparation. When the scattering is linearly anisotropic in angle, the neutron balance equation becomes:

$$\begin{aligned} [\Sigma(E) + i\mathbf{B} \cdot \mathbf{\Omega}] \varphi(E, \mathbf{\Omega}) &= \frac{1}{4\pi} \int_0^{\infty} dE' \\ &\cdot \left\{ \left[ \Sigma_{s,0}(E \leftarrow E') + \frac{\chi(E)}{k} \nu \Sigma_f(E') \right] \Phi(E') + 3\Sigma_{s,1}(E \leftarrow E') \mathbf{\Omega} \cdot \mathbf{J}(E') \right\}, \end{aligned} \quad (7)$$

---

<sup>1</sup> $\delta_{\ell 0}$  is the Kronecker function being equal to 1 if  $\ell = 0$  and zero otherwise.

with the scalar flux  $\Phi = \Phi_0^0 = \int d\Omega \varphi$  and the current  $\mathbf{J} = \int d\Omega \Omega \varphi$ .  $k$  is here a simple parameter normalizing the fission production. We simply set it to 1 and we omit it in the following.

Inversion of the transport operator consists of the multiplication at both sides of Eq. 7 by the factor

$$\frac{1}{\Sigma(E) + i\mathbf{B} \cdot \Omega} = \frac{\Sigma(E) - i\mathbf{B} \cdot \Omega}{\Sigma^2(E) + (\mathbf{B} \cdot \Omega)^2},$$

and integration in angle. Two complex integrals over the unit sphere arise:

$$\frac{1}{4\pi} \int_{4\pi} d\Omega \frac{\Sigma^2}{\Sigma^2 + (\mathbf{B} \cdot \Omega)^2} = \alpha(B, \Sigma)\Sigma, \quad \text{with} \quad (8a)$$

$$\alpha(B, \Sigma) = \frac{1}{B} \cdot \begin{cases} \arctan \frac{B}{\Sigma}, & \text{if } B^2 > 0; \\ \sum_{n=0}^{\infty} \frac{(-1)^{(n)}}{2n+1} \left(\frac{B}{\Sigma}\right)^{(2n+1)}, & \text{if } B/\Sigma \approx 0; \\ \frac{1}{2} \ln \left| \frac{\Sigma+B}{\Sigma-B} \right|, & \text{if } B^2 < 0. \end{cases} \quad (8b)$$

$$\frac{1}{4\pi} \int_{4\pi} d\Omega \frac{(\Omega \otimes \Omega) \cdot \mathbf{B}}{\Sigma^2 + (\mathbf{B} \cdot \Omega)^2} = \beta(B, \Sigma)\mathbf{B}, \quad \text{with} \quad (8c)$$

$$\beta(B, \Sigma) = \frac{1 - \alpha(B, \Sigma)\Sigma}{B^2}. \quad (8d)$$

Special attention is needed when  $B^2$  gets close to zero, which requires to fix some interval around zero to decide when using the series of monomials for numerical evaluation. A singularity arises for negative  $B^2$  when  $B/\Sigma > 1$ , but the integral can be easily regularized. More information about the derivation of these expressions is available in Appendix A. By Eqs. 8, the weighted integration of Eq. 7 yields

$$\begin{aligned} \Phi(E) = & \alpha(B, \Sigma(E)) \int_0^\infty dE' [\Sigma_{s,0}(E \leftarrow E') + \chi(E)\nu\Sigma_f(E')] \Phi(E') \\ & - 3i\beta(B, \Sigma(E)) \int_0^\infty dE' \Sigma_{s,1}(E \leftarrow E') \mathbf{B} \cdot \mathbf{J}(E'). \end{aligned} \quad (9)$$

The result of the previous derivation is combined with the conservation equation obtained by simple integration in angle of Eq. 7:

$$\Sigma(E)\Phi(E) + i\mathbf{B} \cdot \mathbf{J}(E) = \int_0^\infty dE' [\Sigma_{s,0}(E \leftarrow E') + \chi(E)\nu\Sigma_f(E')] \Phi(E'). \quad (10)$$

For parity reasons, we must note that the integral in angle of  $(\mathbf{\Omega} \cdot \mathbf{J})$  vanishes. The scalar product between the vectors  $\mathbf{B}$  and  $\mathbf{J}$  can be replaced in all equations by the term  $(BJ)$ , that is considering only their magnitudes. The substitution of Eq. 9 into Eq. 10 provides after reordering the new equation:

$$\frac{iJ(E)}{B} = \frac{1}{\Sigma\gamma(B, \Sigma)} \left[ \frac{1}{3}\Phi(E) + \int_0^\infty dE' \Sigma_{s,1}(E \leftarrow E') \frac{iJ(E')}{B} \right] \quad (11)$$

$$\text{with } \gamma(B, \Sigma) = \frac{1}{3\Sigma} \frac{\alpha(B, \Sigma)}{\beta(B, \Sigma)} = \sum_{n=0}^\infty c_n \left( \frac{B}{\Sigma} \right)^{2n}. \quad (12)$$

110 The coefficients  $c_n$  are determined by Maclaurin expansions for  $B/\Sigma \rightarrow 0$ :

$$c_1 = \frac{4}{15}, c_2 = -\frac{12}{175}, c_3 = \frac{92}{2625}, c_4 = -\frac{7516}{336875}, \dots$$

Fig. 1 shows the function  $\gamma$  and different approximations of increasing polynomial order obtained by truncating the series expansion. All approximations fit nicely the original function especially close to the origin, and far from it by adding new terms in the sum.

115 The last definition concerns the leakage coefficient, which acts basically as a diffusion coefficient:

$$D(B, E) = \frac{iJ(E)}{B\Phi(E)}. \quad (13)$$

This quantity is always real, with the current  $J$  being purely imaginary or real in case the homogeneous medium is super-critical or sub-critical. Eq. 10 and Eq. 11, with use of Eq. 13, form the system equations to solve for the  
120 homogeneous  $B_1$  model.

#### 4.1. Multigroup Homogeneous $B_1$

As duly noted in Hébert's textbook, this system can be solved using the multigroup energy formalism after choosing a sufficiently large number of groups such that

$$\gamma_g = \int_{E_{g+1}}^{E_g} dE \gamma(B, \Sigma(E)) \approx \gamma(B, \Sigma_g), \quad \forall g.$$

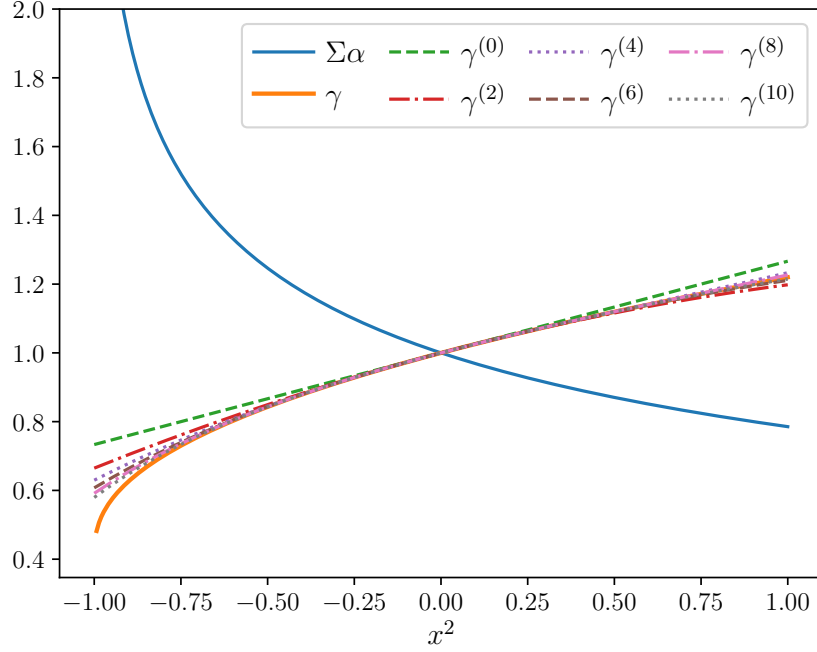


Figure 1: Function  $\gamma$  and its polynomial approximations for increasing degree of  $x^{2n}$ , with  $x = B/\Sigma$ .

The group-dependent data follow as usual:

$$\begin{aligned}\Phi_g &= \int_{E_{g+1}}^{E_g} dE \Phi(E), \\ D_g &= \frac{1}{\Phi_g} \int_{E_{g+1}}^{E_g} dE D(B, E) \Phi(E), \\ \Sigma_g &= \frac{1}{\Phi_g} \int_{E_{g+1}}^{E_g} dE \Sigma(E) \Phi(E).\end{aligned}$$

<sup>125</sup> The leakage rates are  $L_g = D_g B^2 \Phi_g$ ; the coefficients  $D_g B^2$  can be used as additional terms in other transport problems to achieve a critical configuration when preparing homogenized cross sections. The system Eqs. 10 and Eq. 11 can be rewritten in the algebraic multi-group form

$$\left( \vec{\Sigma} + B^2 \vec{D}(B) \right) \odot \vec{\Phi} = (\mathbf{S}_0 + \chi \mathbf{F}) \vec{\Phi} \quad (14a)$$



$$3\vec{\gamma} \odot \vec{\Sigma} \odot \vec{D}(B) \odot \vec{\Phi} = \vec{\Phi} + 3\mathbf{S}_1(\vec{D}(B) \odot \vec{\Phi}) \quad (14b)$$

with a different notation for vectors and matrices in bold. Multiple families  
 130 of fissile nuclides are considered with  $\chi$  and  $\mathbf{F}$ , which contain respectively the  
 emission spectrum and the fission production cross sections of each family  
 per column and per row.  $\mathbf{S}_i$  contains the scattering cross sections of the  $i$ -th  
 anisotropy order. The symbol  $\odot$  indicates the element-wise multiplication  
 (Hadamard product), i.e.  $\vec{D} \odot \vec{\Phi} = \text{diag}(\vec{D})\vec{\Phi}$ . Other products are meant as  
 135 scalar ones if not specified otherwise.

We rearrange the terms in Eq. 14b as:

$$\vec{D} \odot \vec{\Phi} = \frac{1}{3} \left( \text{diag}(\vec{\gamma} \odot \vec{\Sigma}) - \mathbf{S}_1 \right)^{-1} \vec{\Phi}, \quad (15)$$

assuming that the inversion is possible, for substitution in Eq. 14a to obtain:

$$\left[ \left( \text{diag}(\vec{\gamma}(B^2, \vec{\Sigma})) \cdot \mathbf{T} - \mathbf{S}_1 \right) \mathbf{R} + \frac{B^2}{3} \mathbf{I} \right] \vec{\Phi} = 0, \quad (16)$$

with the removal matrix  $\mathbf{R} = \mathbf{T} - \mathbf{S}_0 - \chi\mathbf{F}$ ,  $\mathbf{T} = \text{diag}(\vec{\Sigma})$  and the transport  
 matrix  $\mathbf{\Gamma} = \mathbf{T} - \mathbf{S}_1$ . Still to simplify the notation hereafter, the square-  
 140 bracketed operator in Eq. 16 will be referred to as  $\mathbf{H}(B^2)$ . Eq. 16 constitutes  
 a nonlinear eigenvalue problem where  $B^2$  is an eigenvalue if and only if  $\vec{\Phi}$  is  
 a nontrivial solution.

#### 4.2. The Polynomial Eigenvalue Problem

Eq. 16 shows a non-linear eigenvalue problem to solve. This kind of  
 145 non-linearity can be treated by a proper change of variable in order to get  
 a simpler problem, thanks to the Maclaurin series expansion of the function  
 $\gamma$  in a sum of monomial terms from Eq. 12. The substitution of the series  
 expansion of  $\gamma$  in Eq. 16 yields:

$$\begin{aligned} -\frac{B^2}{3} \vec{\Phi} &= \left[ \left( \sum_{n=0}^{\infty} c_n B^{2n} \mathbf{T}^{-2n} \right) \cdot \mathbf{T} - \mathbf{S}_1 \right] \mathbf{R} \vec{\Phi} \\ &= \left[ \mathbf{\Gamma} + \sum_{n=1}^{\infty} c_n B^{2n} \mathbf{T}^{-(2n-1)} \right] \mathbf{R} \vec{\Phi}, \end{aligned} \quad (17)$$

which is a polynomial eigenvalue problem of infinite order. For completeness,  
 150 a polynomial eigenvalue problem is a problem of the kind (Güttel and Tisseur,

2017):

$$\mathbf{M}(\lambda) \vec{x} = \sum_{m=1}^M \lambda^{(m-1)} \mathbf{M}_m \vec{x} = 0,$$

with  $\vec{x} = [x_g, g = 1, \dots, G]$  and  $\mathbf{M}_m \in \mathbb{C}^{G \times G}$ ,  $\forall m$ . The polynomial order is defined as the number of coefficients needed to write it, practically being equal to its degree plus one. After truncation of the sum to the first  $(N + 1)$  terms, the introduction of the following change of variable:

$$\vec{f}_{n+1} = B^2 \vec{f}_n, \text{ for } n = 0, \dots, N - 1, \text{ with } \vec{f}_0 = \vec{\Phi}, \quad (18)$$

allows to obtain an ordinary linear generalized eigenvalue problem, where the eigenvalue is always  $B^2$  ( $\text{cm}^{-2}$ ). For instance, after neglecting the terms of  $O(B/\Sigma)^8$  the elements in  $\vec{\gamma}$  are approximated by a polynomial of third degree with respect to  $B^2/\Sigma^2$ . The new variables  $\vec{f}_0 = \vec{\Phi}$ ,  $\vec{f}_1 = B^2 \vec{\Phi}$  and  $\vec{f}_2 = B^4 \vec{\Phi}$  are then set in the vector of unknowns  $\vec{f} = [\vec{f}_0, \vec{f}_1, \vec{f}_2]$ , so that a new eigenproblem arises after rearranging the different terms:

$$\begin{pmatrix} \mathbf{T}\mathbf{R} & c_1 \mathbf{T}^{-1} \mathbf{R} & c_2 \mathbf{T}^{-3} \mathbf{R} \\ \mathbf{0} & \mathbf{I} & \mathbf{0} \\ \mathbf{0} & \mathbf{0} & \mathbf{I} \end{pmatrix} \vec{f} = B^2 \begin{pmatrix} -^{1/3} \mathbf{I} & \mathbf{0} & -c_3 \mathbf{T}^{-5} \mathbf{R} \\ \mathbf{I} & \mathbf{0} & \mathbf{0} \\ \mathbf{0} & \mathbf{I} & \mathbf{0} \end{pmatrix} \vec{f}. \quad (19)$$

The fundamental solution of Eqs. 19 can be found by the well-known power method. The derivation of other eigenvalue problems with more terms from the series expansion is straightforward. Besides, the full spectrum of the problem using the polynomial approximation for the function  $\gamma$  can be determined by other general eigenvalue solvers. The rank of these matrices is  $NG$ , where  $G$  is the number of energy groups. They have a few non-zero blocks, and so they lend themselves to storage optimization. Note that the first block at the left top corner of the matrix at the right hand side can be moved to the left hand side with the second block of the first matrix in order to save additional storage.

#### 4.3. Non-linear Inverse Iterations

The transformation adopted in section 4.2 after approximating the transcendental function  $\gamma$  into an algebraic form given by the polynomial expansion changes the eigenproblem in Eq. 16, yielding also a different set of

eigenvalues. It is then necessary to check the convergence of at least the fundamental buckling to the reference value by increasing the truncation order  $N$ . This eigenvalue, that is the fundamental buckling, is always the one with the smallest magnitude.

180 A possible approach to calculate the fundamental eigenvalue is the classical root search combined to the eigenvalue problem of the multiplication factor  $k$ . Specifically, after selecting an initial value of  $B^2$ , the conservation equation is solved by the power method for the eigenvalue  $k$ . A given  $B^2$  value yields specific leakage rates  $L_g$ . The multiplication factor calculated  
185 with these leakage rates will not be equal to 1 in general. So,  $B^2$  is changed according to some root-finding algorithm in order to match the target  $k$  in successive iterations. The power method is used at each iteration to determine the new value of  $k$  until finding the intended  $B^2$  root, which is indeed an eigenvalue of the original problem from Eq. 16.

190 Since we know the operator  $\mathbf{H}$  analytically, we can also use the algorithm based on inverse iterations to get the fundamental solution, see algorithm 1 (Voss, 2013; Güttel and Tisseur, 2017). This algorithm is indeed a variant of Newton's method and the first derivative of the operator on  $B^2$  is needed:

$$\mathbf{H}'(B_i^2) = \text{diag} \left( \vec{\gamma}'(B^2, \vec{\Sigma}) \odot \mathbf{T} \right) \mathbf{R} + \frac{1}{3} \mathbf{I}, \quad (20a)$$

with:

$$\vec{\gamma}' = \frac{1}{B^2} \vec{\gamma} + \vec{f}' \oslash \vec{f} (1 + \vec{f}) \odot \vec{\gamma}, \quad (20b)$$

$$f'_g = -\frac{1}{2B^2} \begin{cases} f_g - \frac{1}{1+x_g^2}, & \text{if } B^2 > 0; \\ \sum_{n=1}^{\infty} (-1)^{(n-1)} \frac{2n}{2n+1} x^{(2n)}, & \text{if } B/\Sigma \approx 0; \\ f_g - \frac{1}{1-x_g^2}, & \text{if } B^2 < 0, \end{cases} \quad (20c)$$

$\vec{f}' = \vec{\Sigma} \odot \vec{\alpha}(B^2, \vec{\Sigma}) = [f_g, g = 1, \dots, G]$  and  $x_g = B/\Sigma_g$ , see Eqs. 8a and 8b.

195 The symbol  $\oslash$  denotes the element-wise division. The functions  $\gamma$  and  $\gamma'$  are plotted in Fig. 2. The function  $\gamma$  shows a cusp point when  $B^2 = -\Sigma$ , being equal to  $1/3$ . At the origin  $\gamma$  and  $\gamma'$  are equal to 1 and  $4/15\Sigma^{-2}$ , respectively.

---

**Algorithm 1** Nonlinear inverse iterations

---

**Require:** Initial pair  $(B_0^2, \vec{\Phi}_0)$  and normalization vector  $\vec{v}$  with  $\vec{v} \cdot \vec{\Phi}_0 = 1$

- 1: **for**  $i = 0, 1, 2, \dots$  until convergence **do**
  - 2:   solve  $H(B_i^2)\vec{\Phi}_{i+1} = H'(B_i^2)\vec{\Phi}_i$  for  $\vec{\Phi}_{i+1}$
  - 3:    $B_{i+1}^2 \leftarrow B_i^2 - (\vec{v} \cdot \vec{\Phi}_i)/(\vec{v} \cdot \vec{\Phi}_{i+1})$
  - 4:   normalize  $\vec{\Phi}_{i+1} \leftarrow \vec{\Phi}_{i+1}/(\vec{v} \cdot \vec{\Phi}_{i+1})$
  - 5: **end for**
- 

## 5. Numerical Results

We present here a simple test case to demonstrate the method with cross  
200 sections condensed in 8 energy groups and homogenized in a  $\text{UO}_2$  fuel pin cell,  
typical of the  $17 \times 17$  AFA 3G fuel assembly used in PWR. All geometrical and  
material specifications follow from Coppolani's textbook (Coppolani, 2012)  
and they are briefly summarized in Table 1. The energy mesh is equi-distant  
in lethargy. The temperature is set uniformly in the coolant, in the cladding  
205 and in the fuel regions. The clad is made of Zircaloy-4 and it is assumed that  
the clad temperature is the same of the coolant as a simplification. 1400 ppm  
of boron are diluted in the coolant, featuring operation at nominal power with  
fresh fuel. Homogenized cross sections are prepared by APOLLO3<sup>®</sup> v2.0.0  
(Schneider et al., 2016) using nuclear data from JEFF3.2.

Table 1: Specifications of the fuel pin cell problem.

Cell pitch	12.588	(mm)
Fuel pellet diameter	8.192	
Inner clad diameter	8.528	
Outer clad diameter	9.500	
Coolant temperature	600	(K)
Fuel temperature	1000	
Linear power	178.00	(W/cm)
Fuel enrichment	3.25	(w/o $^{235}\text{U}$ )
Power per g of HMM	39.70	(W/g)
Coolant pressure	155	(bar)

210 The cross sections of  $^{235}\text{U}$ ,  $^{238}\text{U}$  and  $^{91}\text{Zr}$  are self-shielded by the Livolant-Jeanpierre method (Hébert, 2009), after cell cylindrization keeping the same  
volume of the coolant and using the collision probability method to solve the

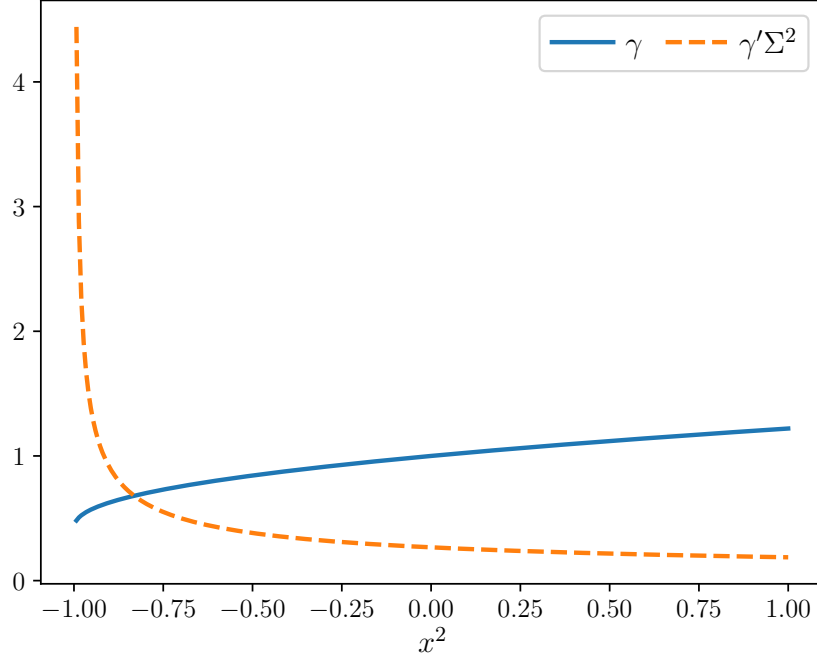


Figure 2: Function  $\gamma$  and its first derivative on  $B^2$ , with  $x = B/\Sigma$

neutron slowing-down problems. Cross sections are spatially homogenized next by the flux obtained with the method of characteristics (MOC) solver.

215 After the change of variable proposed in section 4.1 and the truncation of the series expansion to the  $N$ -th term, we find a linear eigenproblem with  $NG$  eigenvalues in total. The eigenvalues increase in number indeed with higher-order polynomials approximating the function  $\gamma$ . The spectrum of the eigenvalues is shown in Fig. 3 for problems of different truncation orders. The  
 220 eigenvalues obtained with increasing order  $N$  are all different but for the first of smallest magnitude that convergences rapidly to the sought fundamental buckling, see Table 2. The eigenvalues from the eigenproblems obtained by truncating the series expansion of the function  $\gamma$  are not particular samples of the eigenspectrum of the original problem.

225 Table 2 reports the relative differences of the fundamental eigenvalue with the reference one calculated by inverse iterations. The difference in the corresponding eigenvector, that is the fundamental flux, is determined

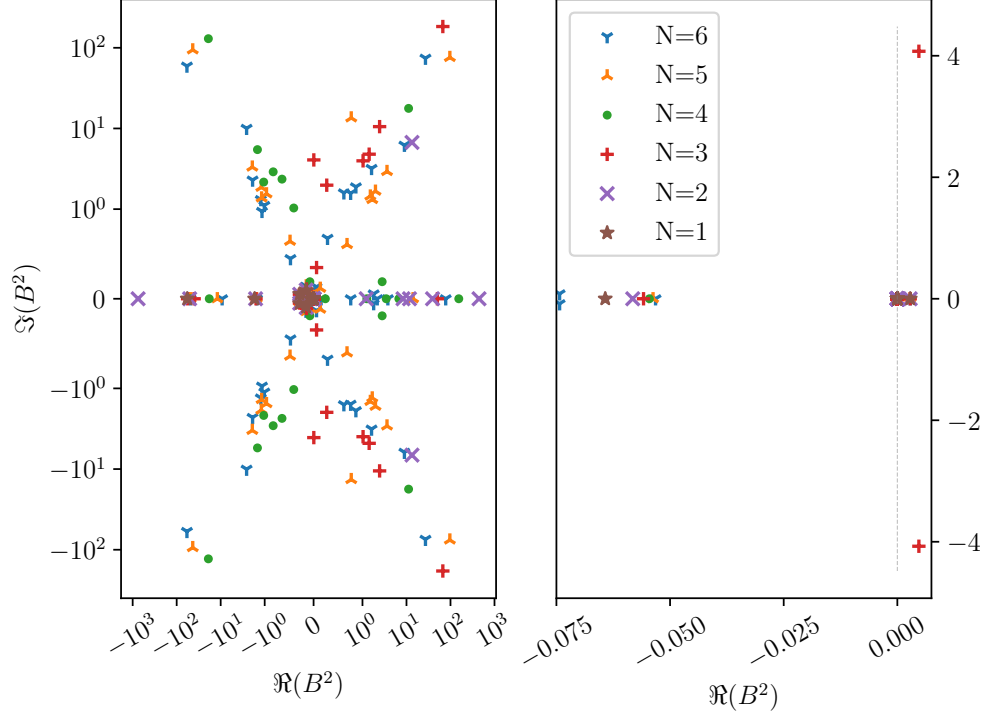


Figure 3: Eigenvalue spectra on the complex plane for different truncation orders; a zoomed-in plot focused near the origin is shown on the right.

by  $e_\Phi = (1 - \vec{\Phi} \cdot \vec{\Phi}_{\text{ref}})$ , where both fluxes have unitary norm.  $N = 3$  is already sufficient to achieve a precision of 6 significant digits. The reference  
 230 solution is provided by nonlinear inverse iterations as explained in section 4.3. Table 3 shows the fundamental buckling and the multiplication factor  $k$  obtained with the corresponding leakage rates. The relative residual errors are determined as:

$$\epsilon_B = |1 - B^{2,(i)} / B^{2,(i+1)}| \quad \text{and} \quad \epsilon_\Phi = \max |1 - \vec{\Phi}^{(i)} \odot \vec{\Phi}^{(i+1)}|.$$

As a matter of comparison, the fundamental solution is also sought by  
 235 the van Wijngaarden-Dekker-Brent method (`brentq` function implemented in the SciPy v1.5.2 library) to seek the root of the function  $k(B^2) = 1$ . This function can be studied numerically and it shows several branches within vertical asymptotes, see Fig. 4. We estimate the asymptote crossing the  $B^2$  axis at the closest point to the origin by resolving the polynomial eigenvalue

240 problem with the factor  $1/k$  set to zero. This allows getting the initial search  
interval, being  $[-0.0216788, 1\text{E}+06]$  with a large enough upper bound. 34  
iterations are necessary to find the solution within the same tolerances used  
for inverse iterations. The method based on inverse iterations proves then to  
be faster than the root search method. All our calculations are performed  
245 by Python v3.8.2 in double-precision floating-point.

Table 2: Convergence of the fundamental buckling  $B^2$  with increasing polynomial degree.

$(2N)$	$B^2$	$e_B$ (%)	$e_\Phi$ (%)
2	0.002833485505	-1.571871E-02	+1.567046E-09
4	0.002833028360	+4.175112E-04	+1.265654E-12
6	0.002833040589	-1.416008E-05	-2.220446E-14
8	0.002833040173	+5.396103E-07	+0.000000E+00
10	0.002833040189	-2.162815E-08	+0.000000E+00
12	0.002833040188	+1.659032E-08	+0.000000E+00

Table 3: Convergence of the fundamental buckling  $B^2$  through inverse iterations.

Its.	$B^2$	$\epsilon_B$	$\epsilon_\Phi$	$k(B^2)$
0	0.00000000000000	-	-	1.1789100550687
1	-0.0159851474737	1.000000E+00	9.913361E+02	5.7270598367870
2	0.0077085166158	3.073700E+00	1.143215E+00	0.7779205239307
3	0.0031326498744	1.460702E+00	1.717592E-01	0.9836219410957
4	0.0028343359989	1.052500E-01	1.128273E-02	0.9999282398946
5	0.0028330402123	4.573838E-04	4.820571E-05	0.9999999986533
6	0.0028330401880	8.583263E-09	9.044694E-10	1.0000000000000
7	0.0028330401880	1.683876E-14	9.992007E-16	1.0000000000000

Other eigenpairs can be calculated with inverse iterations by deflation,  
that is by subtracting the identity matrix multiplied by a given eigenvalue  
to the matrix  $\mathbf{H}$ . The algorithm will then converge to another eigenpair,  
according to the proper basin of attraction into which the initial eigenvalue  
and eigenvector used to start the iterations fall. Actually, we retrieved many  
250 different eigenpairs with the same deflated operator.

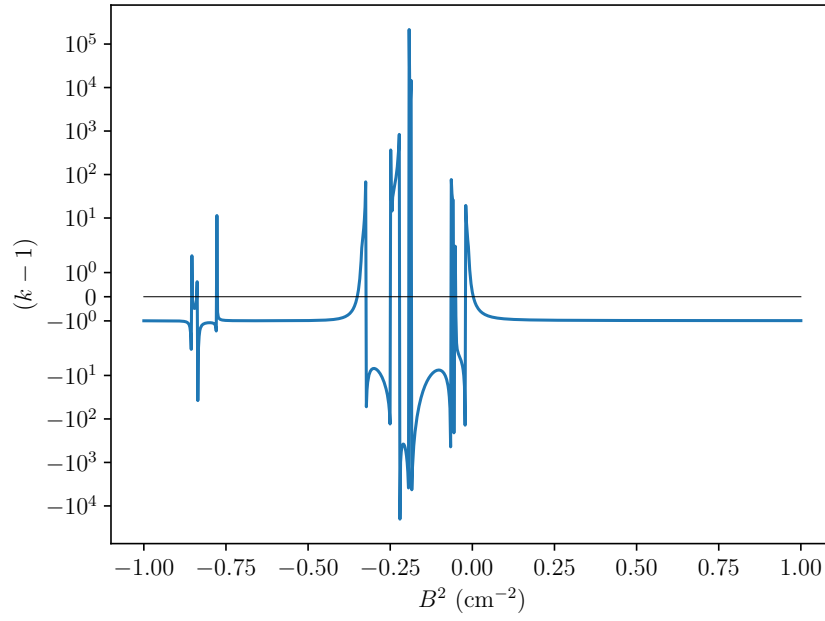


Figure 4: Multiplication factor  $k$  minus 1 as a function of the buckling  $B^2$ .



## 6. Conclusion

This note shows how to transform the non-linear eigenvalue problem for the critical buckling given by the homogeneous  $B_1$  model into an ordinary  
255 linear generalized eigenvalue problem. Contrary to other methods, which are iterative in nature and which are based on root-finding algorithms coupled to the eigenvalue problem of the multiplication factor, this method can obtain the fundamental eigenpair by a single linear generalized eigenvalue problem.

The reference fundamental solution is obtained by nonlinear inverse iterations using the analytical form of the operator associated to the multigroup  
260 neutron balance equation. The methods are demonstrated with a set of cross sections homogenized by APOLLO3<sup>®</sup> in a typical PWR fuel pin cell. The generalization of the technique to any order  $n$  of the homogeneous  $B_n$  theory will be addressed as future research.

## 265 References

- Coppolani, P., 2012. La chaudière des réacteurs à eau sous pression. EDP Sciences. In French.
- Edmonds, A.R., 1996. Angular momentum in quantum mechanics. Princeton university press.
- 270 Güttel, S., Tisseur, F., 2017. The nonlinear eigenvalue problem. Acta Numerica 26, 1–94.
- Hébert, A., 2009. Applied reactor physics. Presses inter Polytechnique.
- Schneider, D., Dolci, F., Gabriel, F., Palau, J.M., Guillo, M., Pothet, B., Archier, P., Ammar, K., Auffret, F., Baron, R., et al., 2016. APOLLO3<sup>®</sup>:  
275 CEA/DEN deterministic multi-purpose code for reactor physics analysis, in: Proc. Int. Conf. PHYSOR2016, Sun Valley, ID, USA, pp. 2274–2285.
- Voss, H., 2013. Nonlinear eigenvalue problems. Chapman and Hall/CRC Boca Raton, FL. In Handbook of Linear Algebra, Ch. 60.

## Appendix A. Solution of the integrals over the unit sphere

280 The expressions of the functions  $\alpha$  and  $\beta$  from section 4 are derived in this section. The inversion of the transport operator and the integration over

the solid angle leads to two integrals of the form:

$$\int_{4\pi} f d\Omega \quad \text{and} \quad \int_{4\pi} f \Omega d\Omega, \quad \text{with} \quad f = \frac{\Sigma - i\mathbf{B} \cdot \boldsymbol{\Omega}}{\Sigma^2 + (\mathbf{B} \cdot \boldsymbol{\Omega})^2}. \quad (\text{A.1})$$

We consider the reference system in spherical coordinates where the polar angle is measured from the  $\mathbf{B}$  vector, whose direction is arbitrary, see Fig. A.5. The function  $f$  depends only the director cosine  $\mu$  thanks to the scalar

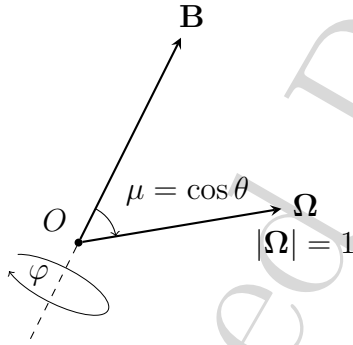


Figure A.5: Spherical reference system with  $\mathbf{B}$  aligned along  $\mu = 0$ ;  $\theta$  and  $\varphi$  are the polar and the azimuthal angles, respectively.

285

product, and these integrals can be split in the different components arising at the nominator which are then solved separately. Some of these integrals vanish because of the odd parity of the corresponding integrand. In the homogeneous leakage model,  $\mathbf{B}$  can only be purely real or imaginary, so that the first non-vanishing integral becomes:

290

$$\frac{1}{4\pi} \int_{2\pi} d\varphi \int_{-1}^1 d\mu \frac{\Sigma}{\Sigma^2 \pm B^2 \mu^2} = \frac{1}{2B} \int_{-B/\Sigma}^{+B/\Sigma} dy \frac{1}{1 \pm y^2}, \quad (\text{A.2})$$

where the sign follows from the complex type of  $\mathbf{B}$ . The change of variable  $y = B\mu/\Sigma$  is used to simplify the integral in A.2. The primitive  $F$  of this rational function is different according to the sign:

$$F = \begin{cases} \arctan y, & \text{if } (+); \\ \frac{1}{2} \ln \left| \frac{1+y}{1-y} \right|, & \text{if } (-). \end{cases}$$

The case of  $|B/\Sigma| \rightarrow 0$  must be treated carefully. We use the asymptotic expansion:

$$\frac{1}{1 - (iy)^2} = \sum_{n=0}^{\infty} (-1)^{(n)} y^{(2n)}$$

to regularize the calculation of the integral in the limit, thus using a polynomial as primitive function. The evaluation of the definite integral with the different primitives yields the expressions reported in Eq. 8b.

From A.1, the only other integrals that do not vanish for odd parity are issued by:

$$-\frac{1}{4\pi} \int_{4\pi} d\Omega \frac{(\mathbf{\Omega} \otimes \mathbf{\Omega}) \mathbf{B}}{\Sigma^2 + B^2 \mu^2}, \quad (\text{A.3})$$

where the dyadic product of  $\mathbf{\Omega} = (\mu, \varphi)$  is:

$$\mathbf{\Omega} \otimes \mathbf{\Omega} = \begin{bmatrix} \mu^2 & \mu\varphi \\ \mu\varphi & \varphi^2 \end{bmatrix}.$$

Three integrals arise for symmetry, and only those of the diagonal terms are non-zero. Because of the definition of the reference frame, we set  $\mathbf{B} = (B, 0)$  since the azimuthal coordinate of  $\mathbf{B}$  is arbitrary. Therefore, there is only one integral left to solve:

$$-\frac{1}{2} \int_{-1}^{+1} d\mu \frac{\mu^2}{\Sigma^2 \pm B^2 \mu^2} = \frac{\Sigma}{2B^3} \int_{-B/\Sigma}^{+B/\Sigma} 1 - \frac{1}{1 \pm y^2} = \frac{1 - \alpha(B, \Sigma)\Sigma}{B^2}. \quad (\text{A.4})$$